AIP Journal of Applied Physics

Integration of thin film giant magnetoimpedance sensor and surface acoustic wave transponder

Bodong Li, Nedime Pelin M. H. Salem, Ioanna Giouroudi, and Jürgen Kosel

Citation: Journal of Applied Physics **111**, 07E514 (2012); doi: 10.1063/1.3678439
View online: http://dx.doi.org/10.1063/1.3678439
View Table of Contents: http://scitation.aip.org/content/aip/journal/jap/111/7?ver=pdfcov
Published by the AIP Publishing

Integration of thin film giant magnetoimpedance sensor and surface acoustic wave transponder

Bodong Li,[1,a)] Nedime Pelin M. H. Salem,[1] Ioanna Giouroudi,[2] and Jürgen Kosel[1]
[1]*Physical Sciences and Engineering Division, King Abdullah University of Science and Technology, 4700 KAUST, Thuwal 23955, Saudi Arabia*
[2]*Institute of Sensor and Actuator Systems, Vienna University of Technology, Vienna, Austria*

(Presented 1 November 2011; received 23 September 2011; accepted 28 November 2011; published online 9 March 2012)

Passive and remote sensing technology has many potential applications in implantable devices, automation, or structural monitoring. In this paper, a tri-layer thin film giant magnetoimpedance (GMI) sensor with the maximum sensitivity of 16%/Oe and GMI ratio of 44% was combined with a two-port surface acoustic wave (SAW) transponder on a common substrate using standard microfabrication technology resulting in a fully integrated sensor for passive and remote operation. The implementation of the two devices has been optimized by on-chip matching circuits. The measurement results clearly show a magnetic field response at the input port of the SAW transponder that reflects the impedance change of the GMI sensor. © *2012 American Institute of Physics*. [doi:10.1063/1.3678439]

I. INTRODUCTION

Remote and passive sensing is of interest for many applications since it neither requires direct physical contact with the sensor nor a power supply at the sensor. Magnetic sensors are particularly attractive for remote operation and were exploited for various applications, e.g., strain, position, or flow rate detection.[1–4] As a relatively new kind of magnetic sensor, the thin film giant magnetoimpedance (GMI) sensor has been extensively studied in the past decade because of its high magnetic field sensitivity, capability of integration in microfabricated devices, as well as the fact that it is driven by an AC current.[5–14] The AC operation provides the possibility to combine GMI thin film sensors with transducers, which respond to RF signals, for example, surface acoustic wave (SAW) devices. SAW devices have been widely used either as sensors or in combination with sensors as a transponder to enable passive and remote operation. In the first case, the SAW device is a one-port device, which measures variations of physical quantities utilizing its inherent sensitivity of the wave propagation velocity to certain environmental parameters. In the second case, the SAW is used as a two-port device, which is electrically loaded by another sensor and, therefore, indirectly affected by the measurand. One-port SAW sensors have been developed to sense physical and chemical quantities such as temperature,[15] pressure,[16] force,[17] chemical liquid,[18] and magnetic field.[19,20] In a one-port magnetic SAW sensor, either the substrate or the interdigital transducers (IDTs) are magnetic field sensitive to affect the propagation velocity or the resonate frequency. With regard to two-port magnetic SAW sensors, one concept was presented previously utilizing a GMI wire and a SAW transponder.[21,22]

In this work, an integrated device consisting of a tri-layer thin film GMI sensor and a SAW transponder is designed, fabricated, and measured. This integrated device is proposed for passive and remote magnetic sensing applications such as implantable devices or harsh environments, while offering the advantages of mass fabrication.

II. METHODS

A. Design

Figure 1(a) shows the concept of the sensor. First, a wireless signal is received by the antenna that is connected to the source IDT (IDT1). After the conversion of the electrical signal to a mechanical wave through the piezoelectric substrate, a Rayleigh wave is propagating to the other end of the sensor, where it is reflected from the reference IDT (IDT2) and load IDT (IDT3). The reflected Rayleigh waves containing the reference and load information are received by the IDT1 and reconverted to the wireless electrical signal, which is then transmitted by the antenna. In this work, a network analyzer was used to simulate the wireless signal source as well as analyze the reflected signals.

The GMI sensor is matched to the output port (IDT3) at the working frequency of the SAW device. As the impedance of the GMI sensor changes with an applied magnetic field, the matching deteriorates, which causes the amplitude of the signal reflected from IDT3 to change. Since the piezoelectric material is quite sensitive to environmental changes, especially the temperature, a reference IDT is used to enable the removal of such influences. Two metallic pads next to the IDTs act as mechanical absorbers and suppress reflections from other structures on the substrate or the edge of the substrate.

The piezoelectric substrate chosen for this application was $LiNbO_3$ (128°, *Y–X* cut), and the IDTs were made of gold. The working frequency and bandwidth for the SAW

a)Author to whom correspondence should be addressed. Electronic mail: bodong.li@kaust.edu.sa.

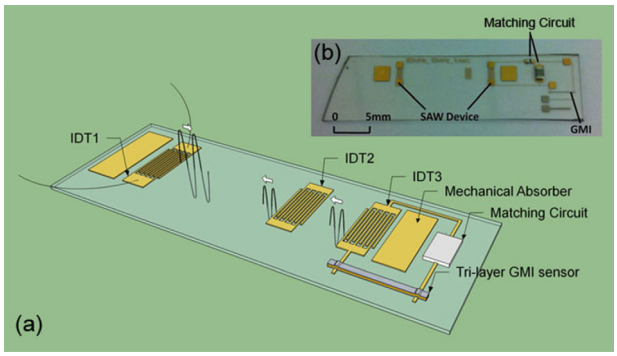

FIG. 1. (Color online) (a) Operation principle of the wireless sensor device. (b) Inset shows a picture of the integrated device.

were designed as 80 MHz, defining the dimensions of the IDTs as follows: $d = 50\,\mu m$ (periodicity of IDT), $FW = 12.5\,\mu m$ (finger-width), $W = 12.5\,\mu m$ (spacing between IDTs). Details on the SAW design can be found elsewhere.[23] The distances between IDTs were $5000\,\mu m$ (from IDT1 to IDT2) and $2500\,\mu m$ (from IDT2 to IDT3). Since the wave velocity is 3994 m/s for $LiNbO_3$, the time the wave requires to travel from IDT1 to IDT2 is $\Delta t_{1,2} = 1.25\,\mu s$ and from IDT2 to IDT3 $\Delta t_{2,3} = 0.625\,\mu s$.

The GMI sensor was designed as a tri-layer structure with a dimension of $100\,\mu m \times 4000\,\mu m$. One 200 nm thick conducting copper layer sandwiched between two 100 nm thick ferromagnetic $Ni_{80}Fe_{20}$ layers formed a GMI structure, which proved effective before for GMI sensors.[24]

B. Fabrication

The fabrication of the combined device was accomplished in several steps as shown in Fig. 2. On a $LiNbO_3$ wafer, a 40 nm Ti adhesion layer and 200 nm gold layer were sputter deposited and then patterned by ion milling into individual SAW devices. The leads and surface mounted device (SMD) footprints were designed together with the SAW device to facilitate an on-chip impedance matching circuit. The GMI sensor material was deposited by e-beam evaporation. A tri-layer structure ($Ni_{80}Fe_{20}$ 100 nm/Cu 200 nm/$Ni_{80}Fe_{20}$ 100 nm) was deposited at room temperature with a 200 Oe constant uni-axial magnetic field applied parallel to the transverse direction of the GMI sensor. After fabrication, two SMD components required for impedance matching were soldered onto the chip. The fabricated device is shown in Fig. 1(b).

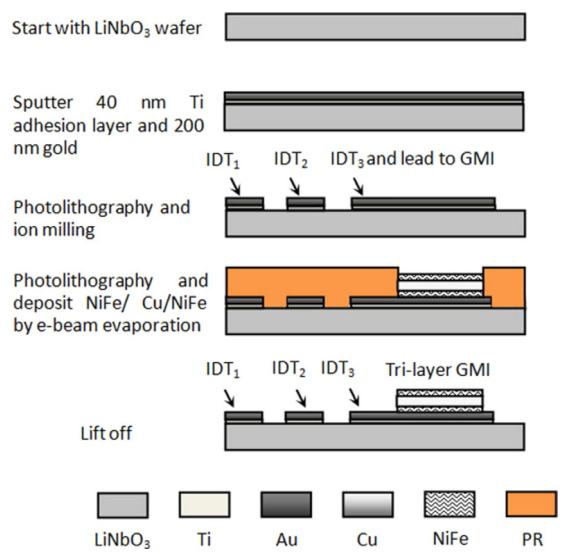

FIG. 2. (Color online) Fabrication flow chart of the integrated SAW-GMI device.

III. GMI RESPONSE

The GMI sensor fabricated for the integrated device has a well-defined transverse magnetic anisotropy and provides high magnetic sensitivity for a wide frequency up to 2 GHz. In order to characterize the GMI sensor, a magnetic field H_{ex} was generated by a Helmholtz coil and applied in the longitudinal direction of the GMI sensor. The GMI ratio is calculated from Z(H) curves defined as GMIratio$= [Z(H_{ex}) - Z(H_0)]/Z(H_0) \times 100\%$, where $Z(H_{ex})$ is the magnetoimpedance with the external magnetic field H_{ex} changing from 0 to 50 Oe. The sensitivity is defined by $\zeta = \{[Z(H_2) - Z(H_1)]/Z(H_1)\}/(H_2 - H_1) \times 100\%$. The magnetic field response of the GMI at 110 MHz measured by an impedance analyzer (Agilent 4294 A) is shown in Fig. 3(a). The most sensitive region of the GMI sensor is around $H_{ex} = 8$ Oe, which is defined by the anisotropy magnetic field observed by VSM [Fig. 3(b)]. The maximum GMI ratio of about 44% and sensitivity of 16%/Oe were also obtained at $H_{ex} = 8$ Oe [Fig. 3(a)]. Those values are very competitive for a tri-layer thin film GMI sensor compared to a GMI ratio of 15% obtained for a similar structure and published recently.[7] The sensitivity (16%/Oe) is in the same range of the GMI wire sensor (100–1200%/mT), which was used previously to integrate with the SAW device.[21] In case of the thin film sensor, the magnetic field region of high sensitivity is lower compared to

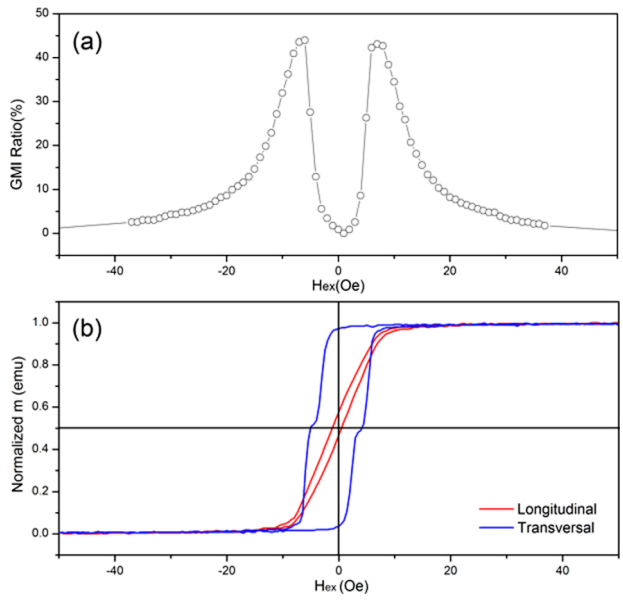

FIG. 3. (Color online) (a) GMI characteristic at 110 MHz. (b) Transversal and longitudinal magnetization curves of the GM sensor.

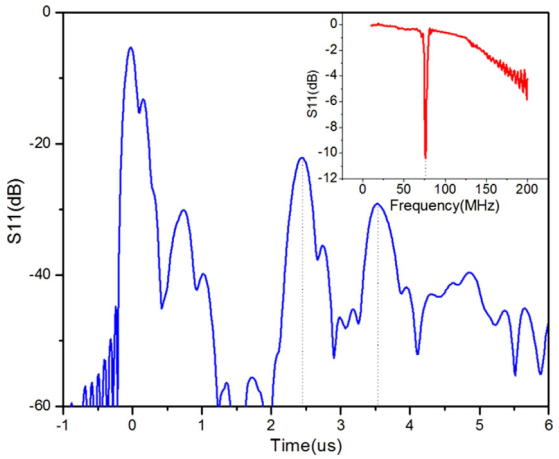

FIG. 4. (Color online) S11 time domain and frequency domain (inset) plot of the integrated device.

the GMI wires, which makes it a better candidate for low field magnetic sensing applications.

IV. SAW CHARACTERISTICS

A network analyzer (Agilent E8363C) was used to analyze the SAW device from both source and load side of the IDT. The S11 of a SAW without any matching circuit or GMI sensor in the frequency range from 10 to 200 MHz is shown in Fig. 4 (inset). There is one major drop at 75 MHz, indicating the working frequency of the integrated device.

V. COMBINED MEASUREMENTS

In order to characterize the integrated device, a time domain measurement was carried out in the frequency range of 65 MHz to 85 MHz (Fig. 4). Two reflection signals were observed at 2.5 μs and 3.5 μs, which correspond to the reference reflection and load reflection. As a response to changes of the external magnetic field, the amplitude of S11 of the load reflection in the time domain changes (Fig. 5). The curve obtained reflects the response of the GMI sensor, with the maximum amplitude of – 29.73 dB measured when the external magnetic field was around 8 Oe.

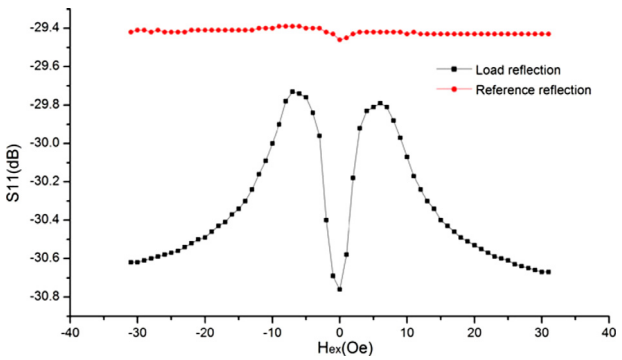

FIG. 5. (Color online) S11 amplitude of the device as a response to an external magentic field.

VI. CONCLUSIONS

A surface acoustic wave device and a thin film giant magnetoimpedance sensor were integrated using standard microfabrication technology. The GMI element has a GMI ratio of 44% and was fabricated on the $LiNbO_3$ substrate together with the SAW transponder. Measurements taken with a network analyzer reflect the response of the GMI sensor to an external magnetic field at the input port of the SAW transponder. A maximum amplitude change of about 1 dB was observed at a field of 8 Oe. As compared to previously reported devices where a GMI wire has been combined with a SAW transponder, the current device can easily be mass fabricated. Future work will focus on improving the frequency response accuracy of the SAW device and make it fully compatible with the GMI sensor.

ACKNOWLEDGMENTS

It is a pleasure to thank Mr. Guodong Li for his help in building the setup of GMI measurements. We also acknowledge the help provided by Mr. Xiang Yu for RF measurements.

[1]E. Sardini and M. Serpelloni, Sensors **9**, 943 (2009).
[2]E. L. Tan, B. D. Pereles, R. Shao, J. Ong, and K. G. Ong, Smart Mater. Struct. **17**, 025015 (2008).
[3]S. Traxler, J. Kosel, H. Pfützner, E. Kaniusas, L. Mehnen, and I. Giouroudi, Sens. Actuators, A **142**, 491 (2008).
[4]J. Kosel, H. Pfützner, L. Mehnen, E. Kaniusas, T. Meydan, M. Vázquez, M. Rohn, A. M. Merlo, and B. Marquardt, Sens. Actuators, A **123**, 349 (2005).
[5]L. V. Paninaand and K. Mohri, Appl. Phys. Lett. **65**, 1189 (1994).
[6]L. V. Panina, K. Mohri, K. Bushida, M. Noda, and T. Uchiyama, IEEE Trans. Magn. **31**, 1249 (1995).
[7]L. Chen, Y. Zhou, C. Lei, and Z.-M. Zhou, Mater. Sci. Eng., B **172**, 101 (2010).
[8]B. Li and J. Kosel, J. Appl. Phys. **109**, 07E519 (2011).
[9]I. Giouroudi, H. Hauser, G. Daalmans, G. Rieger, and J. Wecker, J. Electr. Eng. **55**, 11 (2004).
[10]I. Giouroudi, H. Hauser, L. Musiejovsky, and J. Steurer, J. Appl. Phys. **97**, 10M109 (2005).
[11]F. Blanc-Béguin, S. Nabily, J. Gieraltowski, A. Turzo, S. Querellou, and P. Y. Salaun, J. Magn. Magn. Mater. **321**, 192 (2009).
[12]H. Yang, L. Chen, C. Lei, J. Zhang, D. Li, Z.-M. Zhou, C.-C. Bao, H.-Y. Hu, X. Chen, F. Cui, S.-X. Zhang, Y. Zhou, and D.-X. Cui, Appl. Phys. Lett. **97**, 043702 (2010).
[13]I. Giouroudi, H. Hauser, L. Musiejovsky, and J. Steurer, J. Appl. Phys. **99**, 08D906 (2006).
[14]I. Giouroudi, H. Hauser, L. Musiejovsky, and J. Steurer, IEEE Sens. J. **6**, 970 (2006).
[15]T. M. Reeder and D. E. Cullen, Proc. IEEE **64**, 754 (1976).
[16]K. Lee, W. Wang, G. Kim, and S. Yang, Jpn. J. Appl. Phys., Part 1 **45**, 5974 (2006).
[17]A. Pohl, IEEE Trans. Instrum. Meas. **46**, 1031 (1997).
[18]G. S. Calabrese, H. Wohltjen, and M. K. Roy, Anal. Chem. **59**, 833 (1987).
[19]M. Kadota, S. Ito, Y. Ito, T. Hada, and K. Okaguchi, Jpn. J. Appl. Phys. **50**, 07HD07 (2011).
[20]S. M. Hanna, IEEE Trans. Ultrason. Ferroelectr. Freq. Control **34**, 191 (1987).
[21]H. Hauser, R. Steindl, C. Hausleitner, A. Pohl, and J. Nicolics, IEEE Trans. Instrum. Meas.**49**, 648 (2000).
[22]H. Hauser, J. Steurer, J. Nicolics, L. Musiejovsky, and I. Giouroudi, J. Electr. Eng. **57**, 9 (2006).
[23]H. Al Rowais, B. Li, C. Liang, S. Green, Y. Gianchandani, and J. Kosel, J. Appl. Phys. **109**, 07E524 (2011).
[24]L. V. Panina, K. Mohri, and T. Uchiyama, Physica A **241**, 429 (1997).